PROCEEDINGS OF SCIENCE

Determination of proton parton distribution functions using ATLAS data

Francesco Giuli[*†]

University of Rome Tor Vergata and INFN, Sezione di Roma 2, Via della Ricerca Scientifica 1, 00133 Roma, Italy

E-mail: francesco.giuli@roma2.infn.it

Fits to determine parton distribution functions using top-antitop, inclusive W/Z boson, as well as $W^{\pm}$ boson production measurements in association with jets from ATLAS, in combination with deep-inelastic scattering data from HERA, are presented. The ATLAS W/Z boson data exhibit sensitivity to the valence quark distributions and the light quark sea composition, whereas the top-quark pair production data have sensitivity to the gluon distribution. The impact of the these data is increased by fitting several distributions simultaneously, with the full information on the systematic and statistical correlations between data points. The parton distribution functions extracted using $W^{\pm}$ + jets data show an improved determination of the high-x sea-quark densities, while confirming the unsuppressed strange-quark density at lower $x < 0.02$ found by previous ATLAS analyses.

European Physical Society Conference on High Energy Physics - EPS-HEP2019 -
10-17 July, 2019
Ghent, Belgium

*Speaker.
†on behalf of the ATLAS Collaboration

© Copyright owned by the author(s) under the terms of the Creative Commons Attribution-NonCommercial-NoDerivatives 4.0 International License (CC BY-NC-ND 4.0).

PoS(EPS-HEP2019)478

Introduction A key ingredient of physics with incoming hadrons in the initial state are the Parton Distribution Functions (PDFs), which describes the longitudinal momentum fraction x carried out by partons in a proton. Thus, PDFs represent a fundamental aspect of perturbative QCD phenomenology. High-precision measurements of Standard Model (SM) processes can be used to put constraints on PDFs, allowing comparisons with the current precision reached theoretically. In this document, two different QCD analyses are presented. The first presents the impact of including ATLAS top-quark pair ($t\bar{t}$) production data [1,2], while the second the impact of including ATLAS W^+ and W^- boson production measurements in association with jets [3].

In both these analyses, data are studied in combination with the final neutral-current (NC) and charged-current (CC) deep inelastic scattering (DIS) HERA I+II data [4] and the ATLAS precision measurements of the inclusive differential W and Z/γ^* boson cross sections at $\sqrt{s}$ = 7 TeV [5].

Impact of $t\bar{t}$ cross sections data on PDFs These data are complementary to the W and Z/γ^* boson data in their PDF constraining power since they are sensitive to the high-x gluon distribution ($x \gtrsim 0.05$). They have been measured at 8 TeV using 20.2 fb^{-1} of data in the lepton+jets [1] and dilepton [2] decay modes. While the available spectra in the lepton+jets channel are the invariant mass of the $t\bar{t}$ system, $m_{t\bar{t}}$, the rapidity of the $t\bar{t}$ pair, $y_{t\bar{t}}$, the average top-quark rapidity, y_t^{avg} and the top-quark transverse momentum, p_{T}^t, only the $m_{t\bar{t}}$ and $y_{t\bar{t}}$ spectra are available in the dilepton channel. In the lepton+jets channel, all the available differential spectra have full information on systematic bin-to-bin correlations and the 55 sources of systematic uncertainties are correlated among the different spectra. For the dilepton data the correlations are provided as a total covariance matrix for each spectrum separately, so that only one of these distributions may be fitted at a time. The `xFitter` framework [6] is used for the present QCD analysis, where the PDF evolution is performed using DGLAP at NNLO through `QCDNUM` [7]. Calculations for the W and Z/γ^* boson production are made at NNLO in QCD and NLO in electroweak (EW), while the NNLO predictions of perturbative QCD for top-quark pair production data have recently become available [8].

The initial scale Q_0^2 where PDFs are parametrised as a function of x is chosen to be 1.9 GeV^2, such that it is below the charm mass threshold m_c^2. The heavy quark masses are chosen to be m_c = 1.43 GeV and m_b = 4.5 GeV. The strong coupling constant is fixed to $\alpha_s(M_Z)$ = 0.118. A minimum cut of $Q^2_{\text{min}} \geq 10.0$ GeV^2 is imposed on the HERA data. All these assumptions are varied in the evaluation of model uncertainties on the final fit.

The functional form used for parametrising PDFs is defined as follows:

$$xq_i(x) = A_i x^{B_i}(1-x)^{C_i} P_i(x) \tag{1}$$

where i represents the flavour of the quark distribution, $P_i(x) = (1 + D_i x + E_i x^2)e^{F_i x}$ and the $A_i - F_i$ coefficients are the parameters which are minimized in the fit. The B-parameters determine the low-x behaviour and C-parameters regulate the high-x regime. The chosen PDFs to be parametrised at the starting scale are the gluon distribution, the valence quark distributions, xu_v and xd_v, and the light anti-quark distributions, $x\bar{u}$,$x\bar{d}$ and $x\bar{s}$. A more flexible form, namely $xg(x) = A_g x^{B_g}(1-x)^{C_g} P_g(x) - A'_g x^{B'_g}(1-x)^{C'_g}$ (with $C'_g = 25$ to suppress negative contributions at high-x) is used for parametrising the gluon PDF. The χ^2 used to compare experimental measurements, μ_i, with

PoS(EPS-HEP2019)478

		lepton+jets p_{T}^{t}, $m_{t\bar{t}}$ and dilepton $y_{t\bar{t}}$ spectra
Total χ^2/NDF		1253.8 / 1061
Partial χ^2/NDP	HERA	1149 / 1016
Partial χ^2/NDP	ATLAS $W, Z/\gamma^*$	78.9 / 55
Partial χ^2/NDP	ATLAS lepton+jets p_{T}^{t}, $m_{t\bar{t}}$	16.0 / 15
Partial χ^2/NDP	ATLAS dilepton $y_{t\bar{t}}$	5.4 / 5

Table 1: Total and partial χ^2 for datasets entering the PDF fit to dilepton $y_{t\bar{t}}$ spectrum and the lepton+jets $m_{t\bar{t}}$ and p_{T}^{t} spectra.

theoretical predictions, m_i, is defined as:

$$\chi^2 = \sum_{ij}\left(m_i - \sum_k \gamma_{ki} b_k - \mu_i\right) C^{-1}_{\mathrm{stat\ ij}} \left(m_j - \sum_k \gamma_{kj} b_k - \mu_j\right) + \sum_k b_k^2 \quad (2)$$

where $C_{\mathrm{stat\ ij}}$ represents the statistical correlations between data points i, j and the systematic correlations are treated by nuisance parameters, b_k, for each source of systematic uncertainty k. The 1σ deviation correlated systematic uncertainty on point i due to the systematic uncertainty k is represented by the γ_{ki} quantities, while the $\sum_k b_k^2$ term takes the $\pm 1\sigma$ constraints of the nuisance parameters into account.

A fit to the $m_{t\bar{t}}$ and p_{T}^{t} spectra from lepton+jets and the $y_{t\bar{t}}$ spectrum from the dilepton data has been performed and it is called the ATLASepWZtop18 PDF fit. Table 1 shows the χ^2 for this fit. The gluon PDF distribution before and after the three above-mentioned $t\bar{t}$ spectra are added to the HERA and ATLAS W and Z/γ^* boson data. A significantly harder gluon for $x > 0.1$ and a reduced uncertainty on the gluon PDF in the high-x regime can be observed in Fig 2 (left). Then, additional uncertainties due to possible model and parameterisation biases are evaluated. The model uncertainties include effects related to variations of the charm ($1.37 < m_c < 1.49$ GeV), beauty ($4.25 < m_b < 4.75$ GeV) and top ($172.3 < m_t < 175.0$ GeV) quark masses, of the Q^2_{mim} cut on the data to enter the fit ($7.5 < Q^2_{\mathrm{mim}} < 12.5$ GeV^2) and the value of the starting scale Q_0^2 ($1.6 < Q_0^2 < 2.2$ GeV^2). The parameterisation uncertainties corresponds to the envelope of the results obtained with the following extra parameters added in the functions P_i in Eq. 1: the D_g parameter to the gluon PDF and freeing $B_{\bar{s}}$. Furthermore, the impact of adding both E_g and F_g term to the gluon has been studied and it does not bring any additional modification to the gluon shape. The valence and gluon PDFs with model and parametrisation uncertainties are shown in Fig 1 (right).

QCD analysis of ATLAS $W^{\pm}$ boson production data in association with jets The ATLAS $W^{\pm}$ + jets differential cross sections are based on data recorded in pp collisions at $\sqrt{s}$ = 8 TeV, with a total integrated luminosity of 20.2 fb^{-1} and they are provided in the electron channel only. These data are divided in W^+ and W^- cross sections, and correlations among them are fully considered. Four differential spectra are available: the transverse momentum of the W boson, p_{T}^{W}, the transverse momentum of the leading jet, $p_{\mathrm{T}}^{\mathrm{leading}}$, the absolute rapidity of the leading jet, $|y^{\mathrm{leading}}|$ and the scalar sum of transverse momenta of the electron, all jets with $p_{\mathrm{T}} > 30$ GeV and the missing transverse momentum ($E_{\mathrm{T}}^{\mathrm{miss}}$) in the event, H_{T}. There are 50 sources of correlated systematic uncertainty in common between the different spectra, as well as five sources of uncorrelated systematics,

PoS(EPS-HEP2019)478

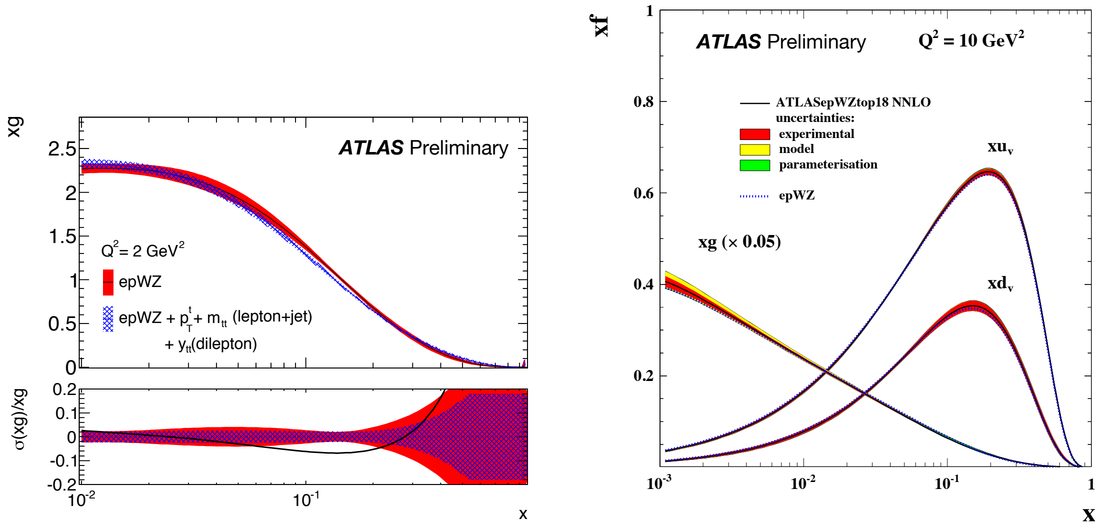

Figure 1: Left: Gluon PDF from a fit to HERA and ATLAS $W, Z/\gamma^*$ boson data plus the lepton+jets $m_{t\bar{t}}$ and p_{T}^t and the dilepton $y_{t\bar{t}}$ compared to a fit to HERA and ATLAS $W, Z/\gamma^*$ boson data only. Only experimental uncertainties on the input data have been included. Right: The valence and gluon PDFs from a fit to HERA and ATLAS W, Z/γ^* boson data plus the lepton+jets $m_{t\bar{t}}$ and p_{T}^t and the dilepton $y_{t\bar{t}}$ are shown, including model and parametrisation uncertainties.

including the data statistics. Moreover, full information on the statistical bin-to-bin correlations in data is available for each spectrum.

As for the previous analysis presented in this document, the `xFitter` fitting framework is used to perform the present QCD analysis. Predictions for $W^{\pm}$ + jets are obtained at fixed order (FO) up to NNLO in QCD and to LO in EW using the $\mathtt{N}_{\text{jetti}}$ program [9]. Outputs from the `APPLGRID` code are used for fast calculations at NLO in QCD and LO in EW, and K-factors to match the before-mentioned $\mathtt{N}_{\text{jetti}}$ predictions are used. The choice of the theoretical input parameters and of the functional form to parametrised PDFs is the same as described in the previous section. A bias correction term, referred to as *log penalty* term, is added to the χ^2 formula in Eq. 2, namely:

$$\sum_i \log \frac{\delta^2_{i,\text{uncor}} T_i^2 + \delta^2_{i,\text{stat}} D_i T_i}{\delta^2_{i,\text{uncor}} D_i^2 + \delta^2_{i,\text{stat}} D_i^2} \tag{3}$$

where D_i represent the measured data, T_i the corresponding theoretical predictions, $\delta_{i,\text{uncor}}$ and $\delta_{i,\text{stat}}$ are the uncorrelated systematic and the statistical uncertainties on D_i. In the following, we will refer to the first term in Eq. 1 as *partial* χ^2, and to the second term as *correlated* χ^2. The statistical correlations considered in this analysis is the bin-to-bin correlations in $W^{\pm}$ + jets data, while there are no statistical correlations considered for the HERA and ATLAS W and Z/γ^* data.

A QCD analysis is then performed, fitting two different $W^{\pm}$ + jets individually, added on top of the HERA and ATLAS W and Z/γ^* data. Fitting more than one $W^{\pm}$ + jets spectrum at a time is not possible, as the spectra are highly correlated to each other, and information on the statistical correlation among them is not available. Tab. 2 shows the total and partial χ^2 per degree of freedom (NDF) for each fit to the $W^{\pm}$ + jets spectra, as well as the correlated component of the χ^2 and the

PoS(EPS-HEP2019)478

Fit	ATLASepWZ19U	ATLASepWZ19U + p_{T}^{W}	ATLASepWZ19U + $p_{\mathrm{T}}^{\mathrm{leading}}$
Total χ^2/NDF	1310 / 1104	1354 / 1138	1365 / 1150
HERA partial χ^2/NDF	1123 / 1016	1132 / 1016	1141 / 1016
HERA correlated χ^2	48	49	50
HERA log penalty χ^2	-18	-22	-25
ATLAS W, Z/γ^* partial χ^2/NDF	117 / 104	116 / 104	109 / 104
ATLAS $W^{\pm}$ + jets partial χ^2/NDF	-	18 / 34	43 / 46
ATLAS correlated χ^2	40	62	47
ATLAS log penalty χ^2	-1	-1	0

Table 2: Total and partial χ^2 for datasets entering the PDF fit, for each $W^{\pm}$ + jets separately, and the ATLASepWZ19U fit.

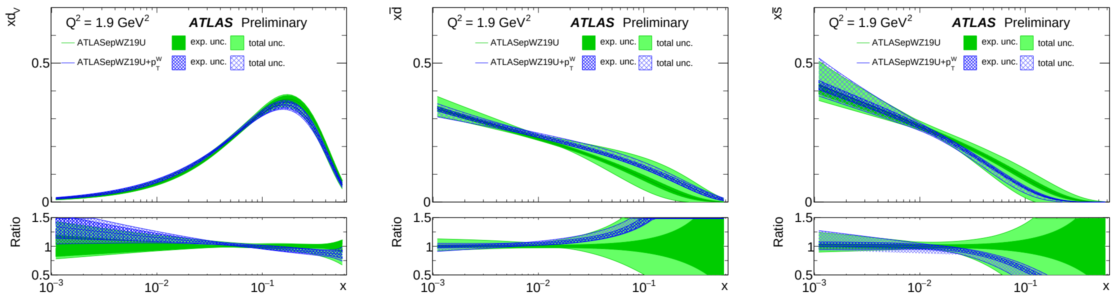

Figure 2: Left: xd_v, Middle: $x\bar{d}$, Right: $x\bar{s}$ PDF obtained when fitting $W^{\pm}$ + jets, inclusive HERA and ATLAS W and Z/γ^* compared to a similar fit without the $W^{\pm}$ + jets data. Inner error bands indicate the experimental uncertainty, while outer bands the total uncertainty, which includes parameterisation and model uncertainties as well.

log penalty term. A good overall fit quality is visible and the partial χ^2 for the HERA and ATLAS W and Z/γ^* data are similar to those obtained in fits to the HERA+ATLAS W, Z data alone. This demonstrate that there is no tension between these data and the $W^{\pm}$ + jets data. Note that the ATLASepWZ19U fit uses the electron and muon decay channels in the W and Z data separately. This choice has been made in order to correlate common sources of systematic uncertainties to those of the $W^{\pm}$ + jets data. Furthermore, this fit has a different Q^2_{min} cutoff and a slightly different PDF parameterisation compared to the original ATLAS PDF fit where these data were included: the so-called ATLASepWZ16 [5].

The PDFs obtained from a fit with the p_{T}^{W} spectrum exhibit the smallest total uncertainty for all parton flavours and the most sensitive distributions are shown in Fig. 2 along with the ATLASepWZ19U fit for comparison. Here, the outer band represent the total uncertainties, which is the sum in quadrature of experimental, model and parameterisation uncertainties. Uncertainties due to model assumptions are evaluated following the same prescription highlighted in the previous section. The uncertainties related to the choice of the PDF parameterisation have been evaluated adding additional parameters separately which give higher flexibility in the high-x regions of all distributions. It has been found that no additional parameters improve the fit χ^2 by more than two, providing fits of similar quality. The resulting PDF set is named “ATLASepWZWjet19”.

As regards the fraction of the strange-quark density in the proton, it can be characterised by the

PoS(EPS-HEP2019)478

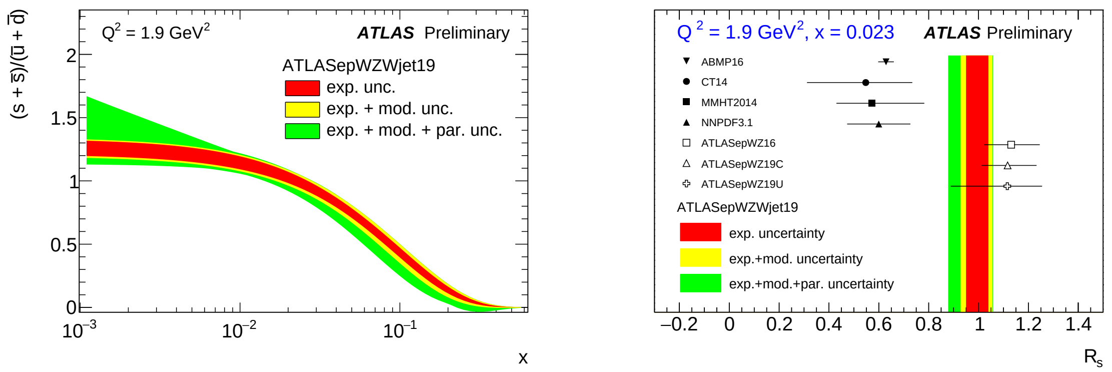

Figure 3: Left: R_s distribution, evaluated at Q^2 = 1.9 GeV^2, predicted by the ATLASepWZWjet19 fit. Right: R_s evaluated at x = 0.023 and Q^2 = 1.9 GeV^2 for the ATLASepWZWjet19 PDF set in comparison to global PDFs [11–14], and the ATLASepWZ16, ATLASepWZ19U and ATLASepWZ16C sets. The experimental, model and parameterisation uncertainty bands are plotted separately for the ATLASepWZWjet19 results. All uncertainty bands are at 68% confidence level.

quantity R_s, defined by the ratio:

$$R_s = \frac{s+\bar{s}}{\bar{u}+\bar{d}} \tag{4}$$

The R_s distribution plotted as a function of x evaluated at Q^2 = 1.9 GeV^2 is shown in Fig.. 3 (left). The uncertainty bands are displayed split in to the experimental, model and parameterisation uncertainties. For $x < 0.023$, the fit with the $W^{\pm}$ + jets data maintains an unsuppressed strange-quark density, compatible with the previous result from the ATLASepWZ16 fit. The new ATLASepWZWjet19 fit favours a lower value of R_s than the ATLASepWZ16 fit, but is consistent to within 1σ and tension remains with the global analyses [11–14] by more than one standard deviations in all cases, as shown in Fig. 3 (right).

Another interesting quantity to look at for judging the performance of PDF sets is the difference between $\bar{d}$ and $\bar{u}$ distributions. The $x(\bar{d}-\bar{u})$ as function of x at Q^2 = 1.9 GeV^2 for the ATLASepWZWjets19 fit is shown in Fig. 4 (left) with an overall positive $x(\bar{d}-\bar{u})$ distribution. This results is in contrast with what previously found in the ATLASepWZ16 fit, as visible in Fig. 4 (right), but it is more in line with what predicted by the global PDF analyses.

References

[1] ATLAS Collaboration. *Measurements of top-quark pair differential cross-sections in the lepton+jets channel in pp collisions at $\sqrt{s}$ = 8 TeV using the ATLAS detector*, *Eur. Phys. J.* **C76** (2016) 538 [hep-ex/arXiv:1511.04716]

[2] ATLAS Collaboration. *Measurement of top quark pair differential cross sections in the dilepton channel in pp collisions at $\sqrt{s}$ = 7 and 8 TeV with ATLAS*, *Phys. Rev.* **D94** (2016) 092003 [hep-ex/arXiv:1607.07281]

[3] ATLAS Collaboration. *Measurement of differential cross sections and W^+/W^- cross-section ratios for W boson production in association with jets at $\sqrt{s}$ = 8 TeV with the ATLAS detector*, *JHEP* **05** (2018) 077 [hep-ex/arXiv:1711.03296]

PoS(EPS-HEP2019)478

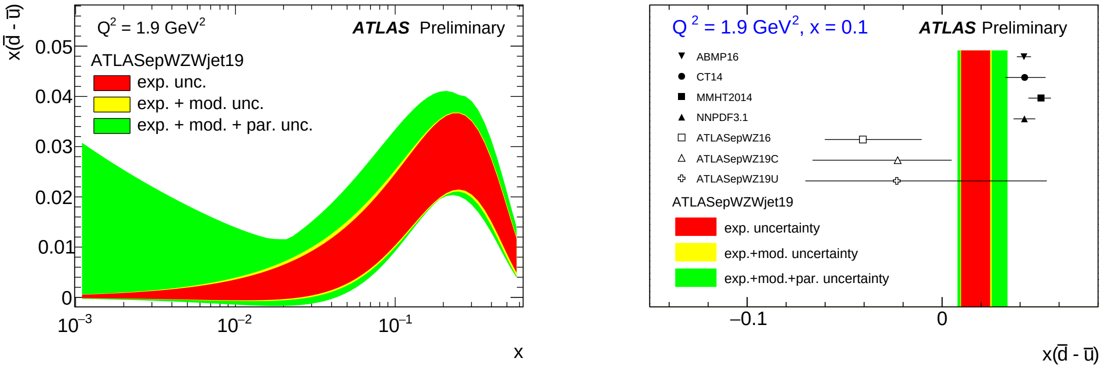

Figure 4: Left: $x(\bar{d}-\bar{u})$ distribution, evaluated at Q^2 = 1.9 GeV^2, predicted by the ATLASepWZWjet19 fit. Right: $x(\bar{d}-\bar{u})$ evaluated at x = 0.1 and Q^2 = 1.9 GeV^2 for the ATLASepWZWjet19 PDF set in comparison to global PDFs [11–14], and the ATLASepWZ16, ATLASepWZ19U and ATLASepWZ16C sets. The experimental, model and parameterisation uncertainty bands are plotted separately for the ATLASepWZWjet19 results. All uncertainty bands are at 68% confidence level.

[4] H1 and ZEUS Collaborations. *Combination of measurements of inclusive deep inelastic $e^{\pm}p$ scattering cross sections and QCD analysis of HERA data*, *Eur. Phys. J.* **C75** (2015) 580 [hep-ex/arXiv:1506.06042]

[5] ATLAS Collaboration. *Precision measurement and interpretation of inclusive W^+, W^- and Z/γ^* production cross sections with the ATLAS detector*, *Eur. Phys. J.* **C77** (2017) 367 [hep-ex/arXiv:1612.03016]

[6] S. Alekhin et al. *HERAFitter*, *Eur. Phys. J.* **C75** (2015) 034 [hep-ph/arXiv:1410.4412]

[7] M. Botje. *QCDNUM: Fast QCD Evolution and Convolution*, *Comput. Phys. Commun.* **182** (2011) 490 [hep-ph/arXiv:1005.1481]

[8] M. Czakon, D. Heymes and A. Mitov. *fastNLO tables for NNLO top-quark pair differential distributions*, (2017) [hep-ph/arXiv:1704.08551]

[9] R. Boughezal, C. Focke, X. Liu and F. Petriello. *W-boson production in association with a jet at next-to-next-to-leading order in perturbative QCD*, *Phys. Rev. Lett.* **115** (2015) 062002 [hep-ph/arXiv:1504.02131]

[10] T. Carti et al. *A posteriori inclusion of parton density functions in NLO QCD final-state calculations at hadron colliders: The APPLGRID Project*, *Eur. Phys. J.* **C66** (2010) 503 [hep-ph/arXiv:0911.2985]

[11] S. Dulat et al. *New parton distribution functions from a global analysis of quantum chromodynamics*, *Phys. Rev.* **D93** (2016) 033006 [hep-ph/arXiv:1506.07443]

[12] L. A. Harland-Lang et al. *Parton distributions in the LHC era: MMHT 2014 PDFs*, *Eur. Phys. J.* **C75** (2015) 204 [hep-ph/arXiv:1412.3989]

[13] The NNPDF Collaboration. *Parton distributions from high-precision collider data*, *Eur. Phys. J.* **C77** (2017) 663 [hep-ph/arXiv:1706.00428]

[14] S. Alekhin et al. *Parton distribution functions, α_S, and heavy-quark masses for LHC Run II*, *Phys. Rev.* **D96** (2017) 014011 [hep-ph/arXiv:1701.05838]

PoS(EPS-HEP2019)478